Numerical Evaluation of Fracture in High-Rise Buildings Subjected to Long Duration Earthquakes

Hashini HERATH
Candidate for the Degree of Master of Engineering
Supervisor: Professor Dr. Taichiro Okazaki
Division of Architectural and Structural Design

Introduction

Subduction zone earthquakes can generate long period, long duration ground motions that can resonate high-rise buildings. There is a serious concern that such load effect can cause a large number of load reversals that lead to fatigue fracture of steel moment connections [1]. This paper presents a numerical study to simulate the response of a typical steel high-rise building including fracture at the connections. Focus is placed on the sensitivity of the analysis results on key material variables.

E-Defense test

Two of the most typical moment connections in early high-rise buildings in the 1970s, the field welded, welded flange-bolted web connection and the shop welded, welded flange-welded web connection were featured in an E-Defense shake table test conducted in 2008 [1]. The specimen, which represented a prototype high-rise building of 21 stories, consisted of a four-story, two span-by-one bay steel moment frame underneath three substitute layers, each comprising a condensated mass, rubber bearings, and a damper as depicted in Fig. 1.

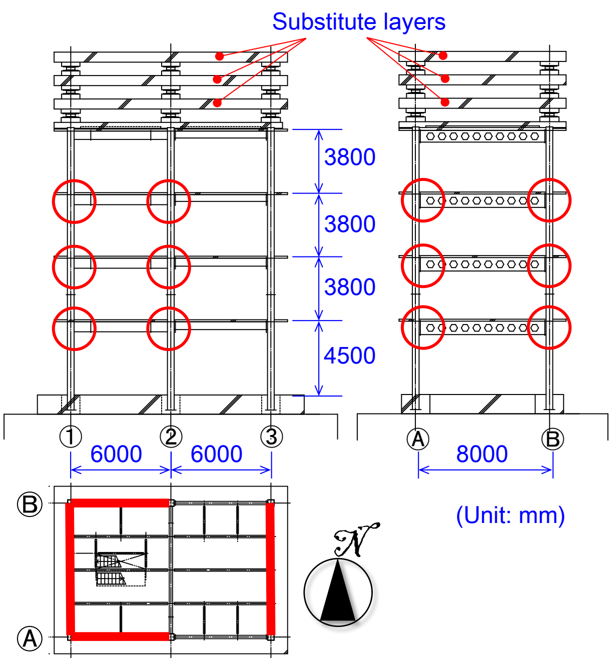

Figure 1. Test frame configuration

The test frame was subjected to increasing magnitudes of ground motions from Level 2 to 3 in Japanese seismic design. The ground motions included El Centro (1940, amplified to PGV of 0.5m/s), Higashi Ogijima (or HOG, a synthesized Tokai earthquake) and Sannomaru (or SAN, a synthesized Tokai-Tonankai earthquake) repeated three times. During the first SAN, three connections in the east frame and one connection in the west frame fractured. After two more SAN repetitions only in the longitudinal direction, two connections in the north frame fractured.

Fracture model

The numerical study used OpenSees, a general-purpose structural analysis framework [2]. OpenSees provides a fatigue material model that assumes a linear damage accumulation in terms of plastic strain and reduces the strength of a fiber to zero when the limit based on Coffin-Manson relationship and Miner's rule is exceeded [3]. Fatigue parameters were calibrated based on constant amplitude, low-cycle fatigue tests on beam-to-column connections [4] that adopted details similar to that used in the E-Defense test frame. Fig. 2 shows the 2D model of the specimen and how closely it reproduced the strength degradation observed in the test. The columns were represented by elastic beam-column elements. The beam was represented by a beam-with-hinges element with a designated plastic hinge segment taken as 1/6 of the element length and 3 integration points along the length.

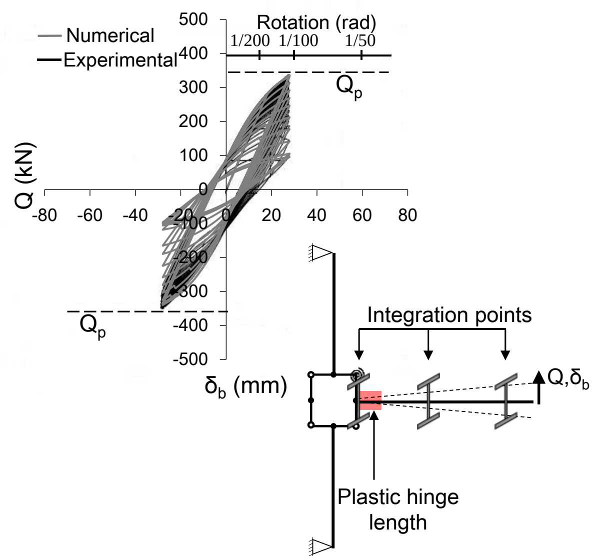

Figure 2. Model for beam-column sub-assemblage

The cross-section was discretized into finer fibers (128) in the hinge region than in the rest of the element (40). Cyclic material property was represented by a Menegotto-Pinto model with combined kinematic and isotropic strain hardening. The parameters were calibrated to result in the best fit to four test results from identical specimens subjected to different loading amplitudes.

Frame model

The longitudinal and transverse frames of the E-Defense test were represented by 2D OpenSees models individually. Fig. 3 shows the numerical model of the longitudinal and transverse frames. Each column was represented by a displacement-based beam-column element with fiber sections at five integration points. Contribution of the concrete floor slabs was included by forming the beam cross-section as a fully composite concrete section above the steel beam section. The castellated beam sections of the transverse frame were expressed by sections with a reduced web thickness. Each beam was represented by a beam with hinges element with fiber sections at six integration points and designated plastic hinge segments at the ends. Properties of steel was modelled by a Menegotto-Pinto model with combined kinematic and isotropic strain hardening, while concrete was modelled by Concrete01 material with zero tensile strength. The fatigue model described above was implemented in the steel section of the beams. Panel zones were assumed to remain elastic as reported from the tests. Condensed concrete mass layers were modelled with rigid elements.

The column bases were modelled as fixed. Floor mass was lumped at the joints in proportion to the tributary floor area. The combined action of steel dampers and rubber bearings were simulated with two node-link elements with equivalent shear springs and rigid axial springs. Rayleigh damping was assumed with a critical damping ratio of 3.5% for the computed first and third vibration periods.

The numerical models were subjected to the same earthquake sequences as the shake table test to account for the phase to phase damage accumulation. The computed vibration modes of the first through third vibration periods in each direction (2.21, 0.84, and 0.56 s in transverse and 2.19, 0.84, and 0.56 s in longitudinal frame) were within 4% of the reported values.

Fig. 4 shows the computed and observed storey drifts of the third and fourth story of the transverse frame along with occurrences of connection fractures during the first SAN excitation. The agreement between the simulated and measured story drift responses was satisfactory. Until multiple connections fractured at about 100s, the vibration

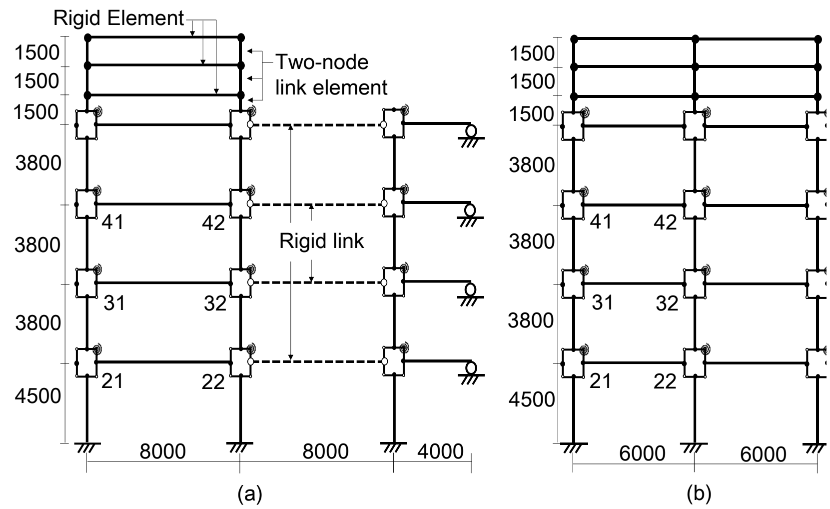

Figure 3. Frame models: (a) Transverse; and (b) Longitudinal (units in mm)

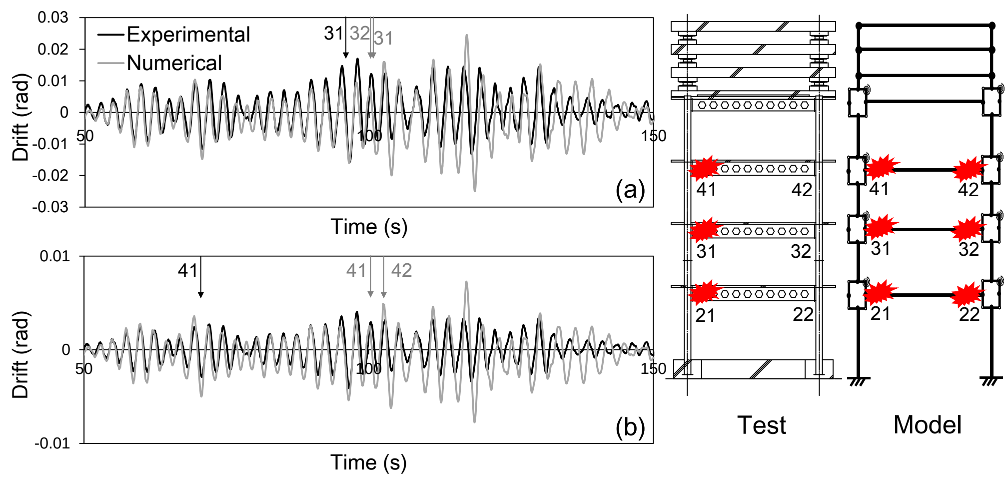

Figure 4. Response of transverse frame: (a) 3rd-story response; (b) 4th-story response

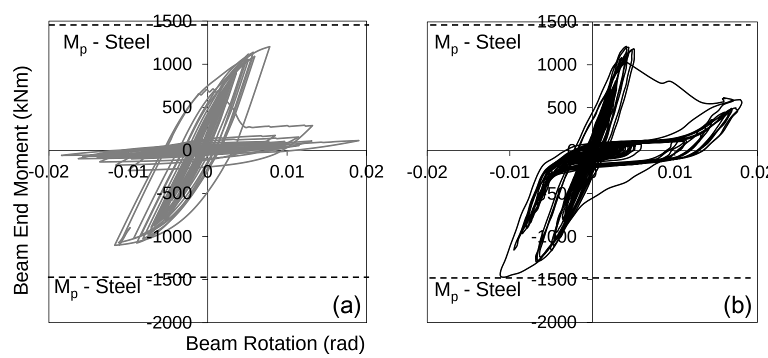

Figure 5. Moment-rotation behavior of connection 31: (a) Numerical response; (b) Experimental response

period matched very well. The timing of fracture was close but not same. (Although not discussed here, connection fractures started much earlier than in the test in the longitudinal frame). In the model, fracture progressed more rapidly and spread more widely, leading to greater elongation of vibration period than the observed. Fig. 5 compares computed versus experimental hysteresis of beam 31, which fractured during the first SAN excitation. The computation reproduced the gradual strength degradation caused by crack initiation and propagation, but the degradation was more rapid than the observed, and the strength in negative bending was smaller. Both test and model responses suggest the beams were unable to develop their plastic strength.

Response sensitivity analysis

Monte Carlo simulations were conducted to examine how the simulation is affected by variability in key properties. In this research, two sources of uncertainty were selected: (1) the fatigue parameters and (2) column-to-beam yield stress ratio. MATLAB, together with OpenSees, was used to conduct these simulations.

Fatigue parameters

Strain amplitude parameter ε_0 of the Coffin-Manson relationship is taken as a random variable with a Gaussian distribution. Fatigue-I stands for a distribution with smaller coefficient of variation that represents the variability observed in the four experimental data points. Fatigue-II tripled the coefficient of variation of Fatigue-I. Fig. 6 shows the two different distributions, controlled by the coefficient of variation for the strain amplitude parameter ε_0. A hundred trials were generated where in each trial, the six connections of interest are provided with a different ε_0 value.

Column to beam yield stress ratio (CBYR)

The variability in yield strength of the columns and beams was addressed by a single parameter, the ratio of yield strength of the columns over that of the beams. The E-Defense specimen used SM490A steel for all beams and columns. Fig. 7 shows the distribution of column-to-beam yield stress ratio computed based on statistical data of SM490A steel.

Five hundred trials were generated with two independent sources of variability, parameter ε_0 of the Coffin-Manson relationship according to Fatigue-I and column to beam yield strength ratio (CBSR). All columns were provided with a fixed yield strength value. The yield strength of the beams was given as the product of the yield strength of the columns and the CBSR for that trial.

The trial results are presented in Fig. 8 in terms of fracture probability of the six connections in transverse and longitudinal frames.

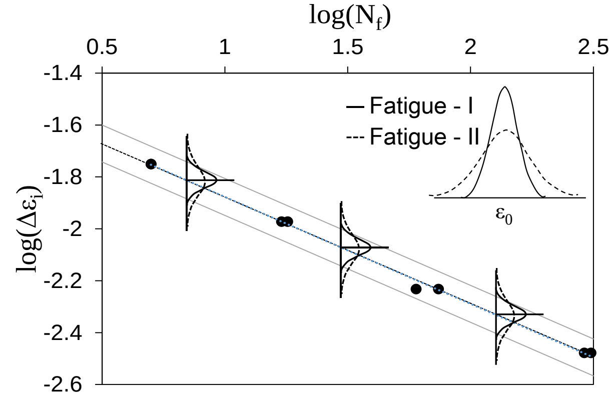

Figure 6. Distribution of fatigue parameters

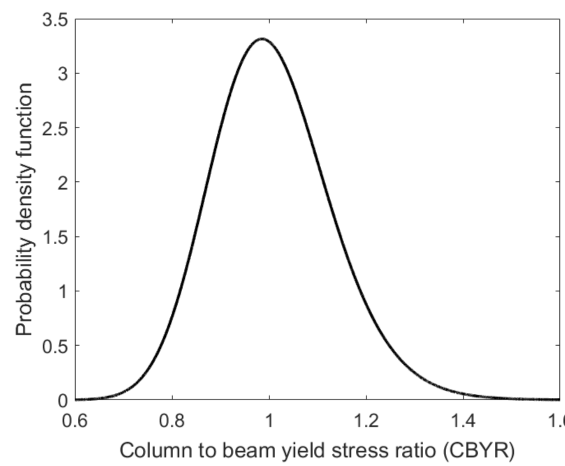

Figure 7. Distribution of CBYR

The simulated response was hardly affected by the fatigue parameter. Interestingly, nearly all connections at the 3rd and 4th floors of both frames fractures for each set of simulation. For Fatigue-I & CBYR, the occurrence of fracture in the longitudinal frame was similar to that obtained from the deterministic approach.

21 Storey model

The same analysis technique was extended to the prototype 21-storey building. The two parallel frames were included in

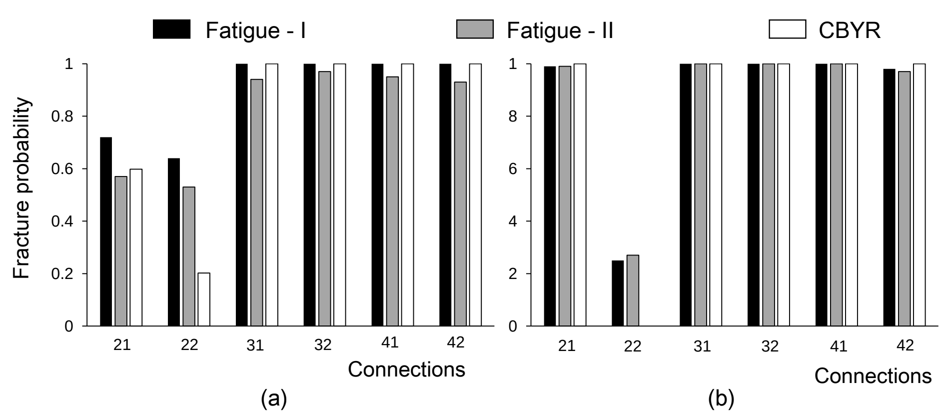

Figure 8. Fracture probability of connections: (a) Transverse frame; (b) Longitudinal frame

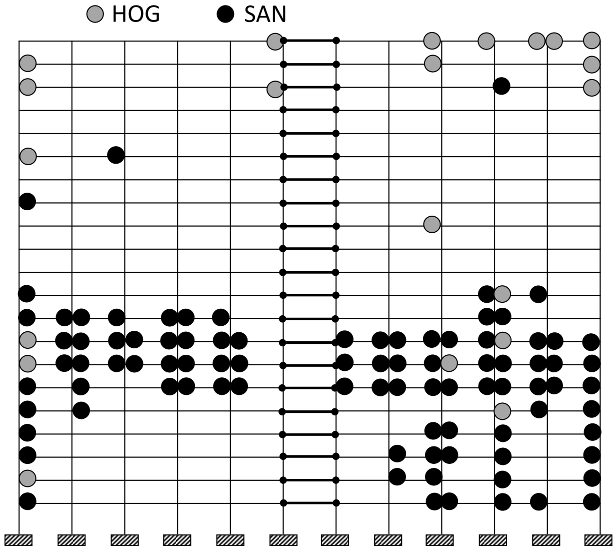

Figure 9. Damage distribution of 21 storey model

the analysis. The beams were modelled using the same element and same discretization as in the E-Defense model. The columns were modelled as displacement-based beam-column elements with five integration points for the first five storeys and by single elastic beam-column elements for the rest of the stories. The same fatigue material model used in the longitudinal frame of the E-Defense frame was implemented in the steel beams. Panel zones were assumed to remain elastic. The model was subjected to the same El Centro, HOG and SAN motions.

The computed vibration modes of the first and second vibration periods 2.32 and 0.83 s were within 6% and 1%, respectively, of the values for the E-Defense frame model. None of the connections fractured during El Centro. Fig.9 illustrates the damage distribution from HOG and SAN. Contrary to the E-Defense model, several connections in the prototype model fractured during HOG. Connection fracture spread widely during SAN. Much of the damage was concentrated in the first 10 floors. Much of the damage to the upper floors were from HOG and very few of them fractured during SAN. Fig. 10 compares the maximum storey drifts obtained from the prototype model and E-Defense model. E-Defense frame model modeled storey shear adequately but was unable to produce the overturning moment. Naturally, the substitute layers could not capture connection fractures at the upper floors, and consequently predicted smaller drift at the upper floors.

Conclusions

A numerical model using OpenSees was developed to simulate the fracture and strength deterioration of steel components due to low cycle fatigue. The model reproduced the experimental behaviour of an E-Defense test specimen adequately. Response sensitivity of the model to the variation of fatigue parameters and column- to- beam yield stress ratio was tested and was found to be minimal. Extending the simulation to the prototype 21 storey building brought out the discrepancies resulted from the contraction process. The two-dimensional modelling approach, which represents fracture progression only along the flange thickness but not along the flange width of steel beams, resulted in a drastic strength deterioration in the steel beam once the fracture initiated. Once a connection fractured at one end of a beam, the other end tended to fracture immediately, thus leading to rapid progression of fractures over the frame.

References

[1.] Okazaki, T. et al.: E-Defense tests on the seismic performance of beam-to-column moment frame connections in high-rise steel buildings, J. Struct. Constr. Eng., AIJ, No. 685, 569-578, Mar., 2013.

[2.] McKenna, F., Object oriented finite element programming frameworks for analysis, algorithms and parallel computing. PhD thesis, University of California, Berkeley, California; 1997.

[3.] Uriz, P., Towards Earthquake Resistant Design of Concentrically Braced Steel Structures, Doctoral Dissertation, Structural Engineering, Mechanics and Materials, Department of Civil and Environmental Engineering, University of California, Berkeley, December 2005

[4.] Hasegawa, T. et al.: Study on seismic performance for super-high-rise steel buildings against long-period earthquake ground motions, BRI Research Data No.161, Building Research Institute, Jul., 2014.

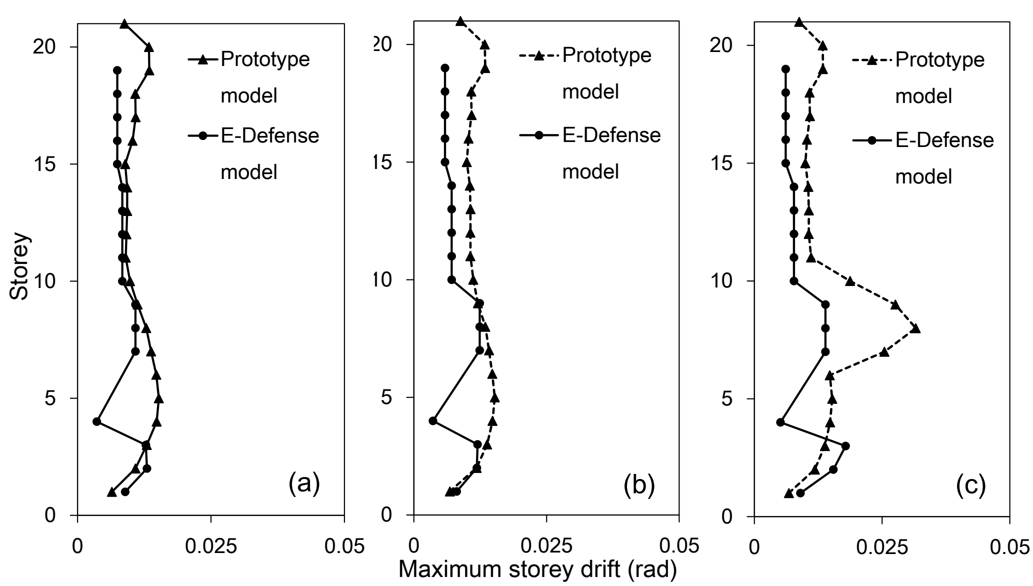

Figure 10. Damage distribution of 21 storey model during: (a) ElCentro; (b) HOG; (c) SAN